

Parameter estimation method for a linear frequency modulation signal with a Duffing oscillator based on frequency periodicity

Ningzhe Zhang(张宁哲), Xiaopeng Yan(闫晓鹏), Minghui Lv(吕明慧), Xiumei Chen(陈秀梅), and Dingkun Huang(黄鼎琨)

Citation: Chin. Phys. B, 2023, 32 (**8**): 080701. DOI: 10.1088/1674-1056/aca206
Journal homepage: http://cpb.iphy.ac.cn; http://iopscience.iop.org/cpb

What follows is a list of articles you may be interested in

Vibrational resonance in globally coupled bistable systems under the noise background

Jiangling Liu(刘江令), Chaorun Li(李朝润), Hailing Gao(高海玲), and Luchun Du(杜鲁春)
Chin. Phys. B, 2023, 32 (**7**): 070502. DOI: 10.1088/1674-1056/acc05f

Synchronization of stochastic complex networks with time-delayed coupling

Duolan(朵兰), Linying Xiang(项林英), and Guanrong Chen(陈关荣)
Chin. Phys. B, 2023, 32 (**6**): 060502. DOI: 10.1088/1674-1056/acc44e

Blind parameter estimation of pseudo-random binary code-linear frequency modulation signal based on Duffing oscillator at low SNR

Ke Wang(王珂), Xiaopeng Yan(闫晓鹏), Ze Li(李泽), Xinhong Hao(郝新红), and Honghai Yu(于洪海)
Chin. Phys. B, 2021, 30 (**5**): 050708. DOI: 10.1088/1674-1056/abd75f

Weak wide-band signal detection method based on small-scale periodic state of Duffing oscillator

Jian Hou(侯健), Xiao-peng Yan(闫晓鹏), Ping Li(栗苹), Xin-hong Hao(郝新红)
Chin. Phys. B, 2018, 27 (**3**): 030702. DOI: 10.1088/1674-1056/27/3/030702

Fast filtering algorithm based on vibration systems and neural information exchange and its application to micro motion robot

Gao Wa (高娃), Zha Fu-Sheng (查富生), Song Bao-Yu (宋宝玉), Li Man-Tian (李满天)
Chin. Phys. B, 2014, 23 (**1**): 010701. DOI: 10.1088/1674-1056/23/1/010701

Parameter estimation method for a linear frequency modulation signal with a Duffing oscillator based on frequency periodicity

Ningzhe Zhang(张宁哲), Xiaopeng Yan(闫晓鹏)†, Minghui Lv(吕明慧), Xiumei Chen(陈秀梅), and Dingkun Huang(黄鼎琨)

Science and Technology on Electromechanical Dynamic Control Laboratory, School of Mechatronical Engineering, Beijing Institute of Technology, Beijing 100081, *China*

(Received 2 August 2022; revised manuscript received 14 October 2022; accepted manuscript online 11 November 2022)

In view of the complexity of existing linear frequency modulation (LFM) signal parameter estimation methods and the poor antinoise performance and estimation accuracy under a low signal-to-noise ratio (SNR), a parameter estimation method for LFM signals with a Duffing oscillator based on frequency periodicity is proposed in this paper. This method utilizes the characteristic that the output signal of the Duffing oscillator excited by the LFM signal changes periodically with frequency, and the modulation period of the LFM signal is estimated by autocorrelation processing of the output signal of the Duffing oscillator. On this basis, the corresponding relationship between the reference frequency of the frequency-aligned Duffing oscillator and the frequency range of the LFM signal is analyzed by the periodic power spectrum method, and the frequency information of the LFM signal is determined. Simulation results show that this method can achieve high-accuracy parameter estimation for LFM signals at an SNR of −25 dB.

Keywords: linear frequency modulation (LFM) signal, Duffing oscillator, frequency periodicity, parameter estimation

PACS: 07.50.Qx, 05.45.–a **DOI:** 10.1088/1674-1056/aca206

1. Introduction

Linear frequency modulation (LFM) signal is a kind of nonstationary signal whose frequency changes linearly with time. Compared with a single-point frequency signal, an LFM signal has a larger time–bandwidth product and better anti-intercept characteristics. It has been widely used in communication, radar, electronic countermeasures and other fields.[1]

Traditional parameter estimation methods for LFM signals mainly focus on time–frequency (TF) domain analysis, such as the short-time Fourier transform (STFT) method, Wigner–Ville distribution (WVD) method and correlation expansion algorithms.[2] However, due to the limitations of time–frequency resolution and cross-terms, these algorithms perform poorly in anti-noise performance.[3,4]

In 2004, Peter O'Shea introduced the cubic phase function (CPF), proposed a parameter estimation method based on the time–chirp rate (TCR) domain, and obtained the statistical estimation results of all parameters with only one-dimensional maximization.[5,6] However, this method can only obtain the asymptotic optimal estimation of a single-component LFM signal under a high signal-to-noise ratio (SNR). Multicomponent LFM signal detection may create cross-terms and spurious peaks. In Ref. [7], the product cubic phase function (PCPF) is used to solve the identifiability problem of spurious peaks and cross-terms by utilizing the different time dependence of cross-terms and auto-terms. Compared with CPF, PCPF has a lower threshold SNR, but the estimation accuracy is slightly reduced. Reference [8] proposed the integrated cubic phase function (ICPF), which makes use of the property that the auto-terms in the CPF are distributed along the straight lines parallel to the time axis in the TCR domain, while the locations of the cross-terms change with time. By integrating over these straight lines, the auto-terms are enhanced, and the cross-terms and spurious peaks are suppressed. On the basis of the ICPF, Ref. [9] further proposed a coherently integrated cubic phase function (CICPF). By coherently integrating the energy of the auto-terms, a −9 dB SNR detection threshold for a single-component LFM signal was achieved. Zheng *et al.*[10] proposed a parameterized centroid frequency–chirp rate distribution (PCFCRD) method for multicomponent LFM signal analysis. By introducing a constant delay, the correlation of noise is reduced, and a better estimation result can be obtained at −12 dB SNR.

Since Almeida[11] proved that fractional Fourier transform (FRFT) can be interpreted as a rotation operator and corresponds to a representation of the signal on an orthonormal basis formed by chirps, FRFT has been widely used in parameter estimation of chirp signals. In 2003, Qi *et al.*[12] realized the detection and parameter estimation of multicomponent LFM signals by using the energy aggregation characteristics of FRFT under different orders. However, this method is essentially a two-dimensional search process with high blindness, and the higher the estimation accuracy is, the greater the amount of calculation needed. Reference [13] proposed an efficient FRFT algorithm. Using the geometric relationship between the FRFT rotation angle and the corresponding nor-

†Corresponding author. E-mail: yanxiaopeng@bit.edu.cn

© 2023 Chinese Physical Society and IOP Publishing Ltd

malized projection length, the optimal rotation angle can be obtained only by two FRFTs, which greatly reduces the calculation time of the algorithm, but the estimation accuracy of the algorithm is difficult to control. On this basis, Ref. [14] accurately searched the best order estimated by the efficient FRFT algorithm, utilizing the better impulse characteristic and noise resistance of the fourth-order origin moment of the signal fractional order spectrum, which improved the estimation accuracy of the algorithm and achieved more accurate estimation results at −10 dB SNR. Reference [15] combined the quadratic phase function (QPF)[5] with FRFT. First, a high-accuracy frequency modulation rate estimate can be obtained from QPF, and then FRFT is used to estimate the other parameters, which shortens the operation time of the algorithm on the premise of ensuring accuracy of parameter estimation. Guo *et al.*[16] proposed a new ℓ^p norm and used Harris hawk optimization (HHO) to search for the optimal FRFT angle, which has good noise resistance and stability.

In this paper, the relationship between periodic signals with different frequencies and the output signals of the Duffing oscillator is analyzed. On this basis, a parameter estimation method for LFM signals is proposed based on the periodic variation characteristic of the output signals of the Duffing oscillator excited by LFM signals with frequency. First, the modulation period is estimated by autocorrelation processing of the output signal of the Duffing oscillator. Second, the relationship between the reference frequency of the frequency-aligned Duffing oscillator and the frequency range of the LFM signal is obtained by the periodic power spectrum method to determine the frequency information of the LFM signal, and then the parameter estimation for the LFM signal can be completed. Due to the inherent high sensitivity of the Duffing oscillator to periodic and quasiperiodic signals and strong immunity to noise,[17] compared with other estimation methods, the method proposed in this paper is more applicable for weak signal detection and has great advantages in a low SNR environment. Simulation results show that stable and high-accuracy parameter estimation results can be obtained when SNR ≥ -25 dB SNR.

2. Duffing oscillator signal detection system

The typical Duffing–Holmes oscillator equation is

$$\ddot{x}(t)+k\dot{x}(t)-x(t)+x^3(t)=F\cos(\omega t), \tag{1}$$

where x is the displacement, t is the time, k is the damping ratio, $-x+x^3$ is the nonlinear restoring force, and $F\cos(\omega t)$ is the internal reference signal. When $k=0.5$ and $\omega=1$ rad/s, the system has obvious nonlinear dynamic characteristics, which can be used for signal detection. To apply to the detection of periodic signals with different frequencies, Equation (1) can be frequency transformed[18] and rewritten into state equations as follows:

$$\begin{cases} \dot{x}=\omega y, \\ \dot{y}=\omega\left(-ky+x-x^3+F\cos(\omega t)\right). \end{cases} \tag{2}$$

If $F=0$, the system will finally stop at one of the two focal points $(-1,\ 1)$ and $(1,\ -1)$. Then, with increasing F, the system will sequentially experience periodic oscillation, homoclinic orbit, period-doubling bifurcation, chaotic state, intermittent chaotic state and large-scale periodic state.[18,19] The traditional Duffing oscillator signal detection method mainly uses the phase state transition of the Duffing oscillator from a chaotic state to a large-scale periodic state. That is, take $F=F_c$; at this time, the system is in a critical chaotic state. If a weak periodic signal with the same frequency is added to the system, the system will be converted from chaotic motion to large-scale periodic motion.

Two periodic signals with amplitude A and frequencies ω_1 and ω_2 $(\omega_1\neq\omega_2)$ are added into the Duffing oscillator model

$$\begin{cases} \ddot{x}_1(t)+k\dot{x}_1(t)-x_1(t)+x_1^3(t) \\ =F\cos(\omega t)+A\cos(\omega_1 t), \\ \ddot{x}_2(t)+k\dot{x}_2(t)-x_2(t)+x_2^3(t) \\ =F\cos(\omega t)+A\cos(\omega_2 t), \end{cases} \tag{3}$$

$$\begin{aligned} &\left(\ddot{x}_1(t)-\ddot{x}_2(t)\right)+k\left(\dot{x}_1(t)-\dot{x}_2(t)\right) \\ &-\left(x_1(t)-x_2(t)\right)+\left(x_1^3(t)-x_2^3(t)\right) \\ &=A\left(\cos(\omega_2 t)-\cos(\omega_1 t)\right). \end{aligned} \tag{4}$$

Taking $x(t)=x_1(t)-x_2(t)$, $\dot{x}(t)=\dot{x}_1(t)-\dot{x}_2(t)$, $\ddot{x}(t)=\ddot{x}_1(t)-\ddot{x}_2(t)$, Eq. (4) can be expressed as

$$\begin{aligned} &\ddot{x}(t)+k\dot{x}(t)-x(t)+x^3(t)+3x_1x_2x \\ &=A\left(\cos(\omega_2 t)-\cos(\omega_1 t)\right). \end{aligned} \tag{5}$$

Substituting Eq. (1) into Eq. (5), we obtain

$$F\cos(\omega t)+3x_1x_2x=A\left(\cos(\omega_2 t)-\cos(\omega_1 t)\right), \tag{6}$$

$$3x_1x_2x=A\left(\cos(\omega_2 t)-\cos(\omega_1 t)\right)-F\cos(\omega t). \tag{7}$$

Because $\omega_1\neq\omega_2$, $A\left(\cos(\omega_2 t)-\cos(\omega_1 t)\right)-F\cos(\omega t)\neq 0$. Therefore, $3x_1x_2x\neq 0$, $x_1\neq 0$, $x_2\neq 0$, and $x\neq 0$.

We can obtain $x_1\neq x_2$; that is, when the frequencies of the input periodic signals are different, the output signal of the Duffing oscillator is also different.

Figure 1 shows the time domain diagrams of Duffing oscillator output signals when inputting periodic signals with different frequencies. For convenience of observation, we set $k=0.5$, the Duffing oscillator internal reference frequency $\omega=2\pi f$, $f=100$ MHz, $F=F_c=0.8259$, the frequency of the input periodic signal $f_0=35$ MHz, 75 MHz, 100 MHz, 125 MHz, and 165 MHz, and $A=1$ V.

Figure 1 shows the difference in frequency between the internal reference signal and the periodic signal with varying

frequency of the input periodic signal; the Duffing oscillator shows different motion states. Therefore, there is a certain relationship between the output signal of the Duffing oscillator and the difference frequency, which is related to the value and sign of the difference frequency. Figure 2 shows the numerical solution obtained when inputting periodic signals with the same amplitude is shown. Here, we set $k = 0.5$, $f = 100$ MHz, $F = F_c = 0.8259$, $f_0 = 10 \sim 200$ MHz, and $A = 1$ V.

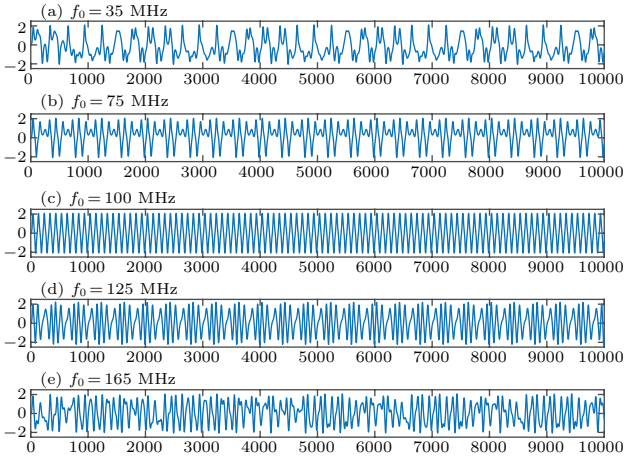


Fig. 1. Output time domain diagrams of the Duffing oscillator excited by periodic signals with different frequencies. Input periodic signal frequency (a) $f_0 = 35$ MHz; (b) $f_0 = 75$ MHz; (c) $f_0 = 100$ MHz; (d) $f_0 = 125$ MHz; (e) $f_0 = 165$ MHz.

In summary, the periodic signals with different frequencies correspond to the different output signals of the Duffing oscillator.

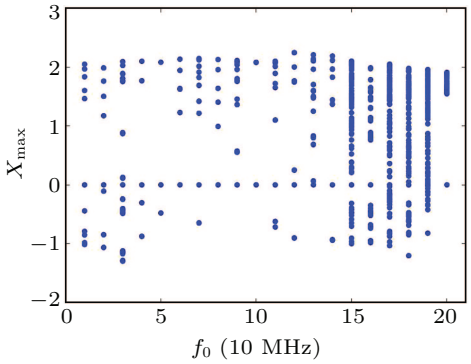


Fig. 2. Numerical solution of the Duffing oscillator excited by periodic signals with different frequencies.

3. Parameter estimation method for an LFM signal with a Duffing oscillator based on frequency periodicity

3.1. Periodic characteristics of the Duffing oscillator excited by the LFM signal

When the Duffing oscillator is excited by the LFM signal, if the influence of noise is ignored, its detection model can be expressed as

$$\begin{cases} \dot{x} = \omega y, \\ \dot{y} = \omega(-ky + x - x^3 + F\cos(\omega t + \varphi) + u(t)), \end{cases} \tag{8}$$

where $u(t)$ is the input LFM signal. Taking the triangular wave LFM signal as an example, its expression[20] is

$$u(t) = \begin{cases} A\cos 2\pi(f_0 t + k_f t^2), & nT_M - T_M/4 < t \le nT_M + T_M/4, \\ A\cos 2\pi(f_0 t - k_f(t - T_M/2)t), & nT_M + T_M/4 < t \le nT_M + 3T_M/4, \end{cases} \tag{9}$$

where A is the signal amplitude, f_0 is the signal center frequency, T_M is the modulation period, $k_f = 2\Delta F_M/T_M$ is the frequency change rate, and ΔF_M is the frequency modulation deviation. For the convenience of analysis, the frequency modulation deviation is set equal to the modulation bandwidth; then, the origin frequency of the LFM signal is $f_{start} = f_0 - \Delta F_M/2$, and the termination frequency is $f_{end} = f_0 + \Delta F_M/2$.

At this time, the frequency difference between the internal reference signal and the detected LFM signal is $|\Delta\omega| = |\omega - \omega_0| = 2\pi|f - (f_0 + k_f t)|$. Because the frequency of the LFM signal changes rapidly with time and the variation range is usually much larger than 0.03ω,[21–24] it is difficult to directly measure the frequency of the LFM signal by using the phase transition of the Duffing oscillator from a chaotic state to a large-scale periodic state. However, for the LFM signal, the frequency changes periodically with time, as does the frequency difference between it and the internal reference signal. Therefore, combined with the one-to-one correspondence between the periodic signals with different frequencies and the output signals of the Duffing oscillator analyzed in Section 2, the modulation period can be estimated using the periodic change characteristics of the frequency of the LFM signal.

Taking the origin frequency of the LFM signal as $\omega_{start} = 2\pi f_{start}$, the termination frequency is $\omega_{end} = 2\pi f_{end}$. According to the frequency relationship between the Duffing oscillator internal reference signal and the LFM signal, it can be divided into five cases. Figure 3 shows the Duffing oscillator output signals under different conditions. We also fix $k = 0.5$ and $F = F_c = 0.8259$ and only change the Duffing oscillator internal reference frequencies $f = 75$ MHz, 100 MHz, 125 MHz, 150 MHz, and 175 MHz. For the input LFM signal, $A = 1$ V, $k_f = 10^4$ GHz·s^{-1}, $f_{start} = 100$ MHz, and $f_{end} = 150$ MHz.

Figure 3 shows the following outcomes. (1) When $\omega < \omega_{start}$ or $\omega > \omega_{end}$, because the frequency of the input LFM signal constantly changes within $[\omega_{start}, \omega_{end}]$, the Duffing oscillator reference signal frequency ω is always outside the frequency range of the LFM signal, and the phase transition condition in which the Duffing oscillator transitions from a

chaotic state to a periodic state cannot be satisfied. Therefore, the Duffing oscillator is always in a chaotic state. (2) When $\omega = \omega_{\text{start}}$ or $\omega = \omega_{\text{end}}$, with a continuous change in the LFM signal frequency, the Duffing oscillator reference frequency will be equal to the LFM signal frequency. Therefore, there is a period of time Δt, in which the difference frequency $|\Delta\omega| \leq 0.03\omega$, and the Duffing oscillator will undergo large-scale periodic motion. If $\omega = \omega_{\text{start}}$, periodic motion occurs between every two modulation cycles; for $\omega = \omega_{\text{end}}$, periodic motion occurs in the middle of each modulation period. (3) When $\omega_{\text{start}} < \omega < \omega_{\text{end}}$, it is similar to analysis (2), except that the reference frequency and the LFM signal frequency are aligned twice in each modulation cycle. Therefore, the modulation period can be estimated by using the periodic change in the output signal of the Duffing oscillator.

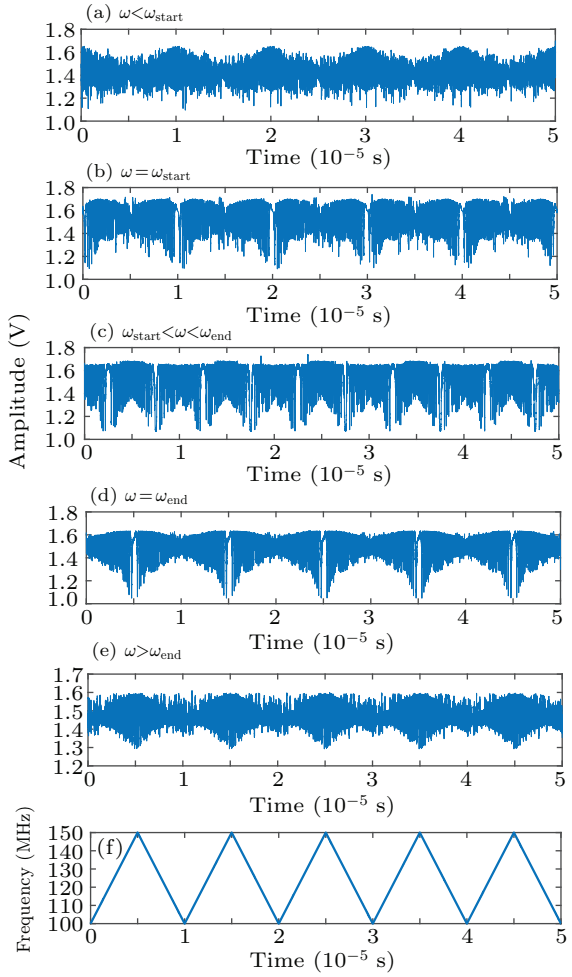


Fig. 3. Input LFM signal and output envelope signals of the Duffing oscillator under different frequency relationships. (a) $\omega < \omega_{\text{start}}$; (b) $\omega = \omega_{\text{start}}$; (c) $\omega_{\text{start}} < \omega < \omega_{\text{end}}$; (d) $\omega = \omega_{\text{end}}$; (e) $\omega > \omega_{\text{end}}$; (f) time–frequency representation of the LFM signal.

From the above analysis, if autocorrelation processing is performed on the output signal of the Duffing oscillator, there may be three results, as shown in Fig. 4.

(1) Taking $\omega_{\text{mid}} = (\omega_{\text{start}} + \omega_{\text{end}})/2$, when $0.9\omega_{\text{mid}} \leq \omega \leq 1.1\omega_{\text{mid}}$, because the frequency of the LFM signal is aligned twice with the reference frequency of the Duffing oscillator in a single modulation period, the autocorrelation function will show a half-periodic characteristic; that is, the average value of the interval between the two adjacent local maximum points is approximately half of the modulation period, as shown in Fig. 4(a). However, with a decrease in the input signal amplitude, this half-periodic characteristic will be rapidly replaced by the periodic characteristic, as shown in Fig. 4(b). When the SNR decreases, the periodic characteristic gradually disappears, as shown in Fig. 4(c).

(2) When $\omega_{\text{start}} \leq \omega < 0.9\omega_{\text{mid}}$ or $1.1\omega_{\text{mid}} < \omega \leq \omega_{\text{end}}$, the output signal shows good periodic characteristics, as shown in Fig. 4(b). In the same way, the periodic characteristic also disappears as the SNR decreases, as shown in Fig. 4(c).

(3) When $\omega < \omega_{\text{start}}$ or $\omega > \omega_{\text{end}}$, although the Duffing oscillator maintains chaotic motion from beginning to end, the amplitude of its output signal will decrease with an increase in the difference frequency, and the degree of chaos of the system will also change. The Duffing oscillator output signal still shows periodic variation characteristics. After autocorrelation processing, the modulation period can be obtained, as shown in Fig. 4(b). However, this periodic characteristic is not only related to the SNR but also shows a strong correlation with the amplitude of the input signal. When the input signal is very weak, it no longer shows periodic characteristics, as shown in Fig. 4(c).

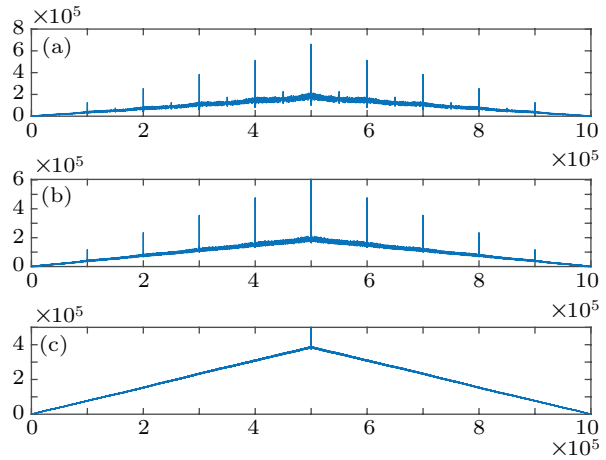


Fig. 4. Autocorrelation function of the Duffing oscillator output signals under different conditions: (a) the half-periodic characteristic; (b) the periodic characteristic; (c) the others.

We set $k = 0.5$, $F = F_{\text{c}} = 0.8259$, $k_{\text{f}} = 10^4$ GHz·s^{-1}, $f_{\text{start}} = 100$ MHz, and $f_{\text{end}} = 150$ MHz. Table 1 shows the influence of the amplitude of the input triangular wave LFM signal on the autocorrelation function under different conditions. Table 1 shows that the emergence of the half-periodic characteristic depends strongly on the strength of the detected LFM signal. When the amplitude of the input detected LFM signal is less than 0.42 V, the half-periodic characteristic will disappear, so it cannot be used for the detection of weak signals.

Table 1. Influence of the detected signal amplitude on the autocorrelation function.

ω	Amplitude of input LFM signal with a noise free background (V)									
	1.5	0.5	0.42	0.41	0.1	0.05	0.04	0.01	0.009	0.008
$0.9\omega_{\text{mid}} \le \omega \le 1.1\omega_{\text{mid}}$	Half[a]	Half	Half	Cycle[b]	Cycle	Cycle	Cycle	Cycle	Cycle	None[c]
$\omega_{\text{start}} \le \omega < 0.9\omega_{\text{mid}}$ or $1.1\omega_{\text{mid}} < \omega \le \omega_{\text{end}}$	Cycle	Cycle	Cycle	Cycle	Cycle	Cycle	Cycle	Cycle	Cycle	None
$\omega < \omega_{\text{start}}$ OR $\omega > \omega_{\text{end}}$	Cycle	Cycle	Cycle	Cycle	Cycle	None	None	None	None	None

[a]The half-periodic characteristic as shown in Fig. 4(a). [b]The periodic characteristic as shown in Fig. 4(b).
[c]The characteristic disappears, as shown in Fig. 4(c).

Table 2. Influence of the SNR on the autocorrelation function.

ω	SNR (dB)							
	0	−10	−16	−17	−18	−20	−27	−28
$\omega_{\text{start}} \le \omega \le \omega_{\text{end}}$	Cycle	Cycle	Cycle	Cycle	Cycle	Cycle	Cycle	None
$\omega < \omega_{\text{start}}$ or $\omega > \omega_{\text{end}}$	Cycle	Cycle	Cycle	None	None	None	None	None

Fixing the amplitude of the input signal as $A = 0.05$ V, the autocorrelation function no longer has half-periodic characteristics, so the above two cases (1) and (2) can be combined into one, i.e., $\omega_{\text{start}} \le \omega \le \omega_{\text{end}}$. Table 2 shows the influence on the autocorrelation function of the Duffing oscillator output signal excited by the triangular wave LFM signal under different SNRs.

The Duffing oscillator excited by the sawtooth LFM signal has frequency alignment at most once in a modulation period, so it only has periodic characteristics, not half-periodic characteristics. Only the influence of the input SNR on the autocorrelation function needs to be considered. Similar to the triangular wave LFM signal, when the input SNR is low, only in the case of $\omega_{\text{start}} \le \omega \le \omega_{\text{end}}$ does the autocorrelation function show periodic characteristics.

3.2. Parameter estimation method for LFM signals based on frequency periodicity

Based on the frequency periodicity analyzed in Subsection 3.1, the modulation period of the LFM signal can be obtained by the autocorrelation function of the Duffing oscillator output signal. Because the half-period characteristic depends strongly on the strength of the input LFM signal and the frequency range of the LFM signal cannot be completely covered, it is greatly limited. Therefore, this paper mainly uses the periodic characteristic of the autocorrelation function to estimate the parameters of the weak LFM signal; that is, the modulation period T_{M} is calculated from the interval between the adjacent local maximum points of the autocorrelation function.

Combined with the analysis in Subsection 3.1, when the reference signal frequency of the Duffing oscillator is within the frequency variation range of the LFM signal, $\omega_{\text{start}} \le \omega \le \omega_{\text{end}}$, the signal always occurs for a period of time Δt in each modulation period, making the difference frequency $|\Delta\omega| \le 0.03\omega$ when the Duffing oscillator moves periodically. Generally, the power spectrum of a chaotic signal has many peaks, which are distributed widely and continuously, and the peak value is small, while for the periodic signal, it contains fewer peaks, with a concentrated distribution and high peaks. Therefore, the power spectrum method can be used to distinguish the signal state. We can adopt the method in which the output signal is divided into several sections, and then the maximum estimated value of the power spectrum of each finite length signal can be calculated. If there is a finite length signal x_n in a modulation period whose power spectrum estimated value is much larger than that of the other finite length sign $x\ldots x_{n-2}, x_{n-1}, x_{n+1}, x_{n+2}\ldots$, it can be preliminarily considered that this section signal corresponds to the periodic motion state of the Duffing oscillator. Of course, chaotic state signals may also have large peaks, but these peaks are usually irregular, much smaller than those of periodic signals, and may occur at any position in a modulation period. Therefore, the chaotic state and periodic state can be discriminated twice by the interval between the occurrence of the maximum estimated value of the power spectrum to reduce the probability of false judgment.

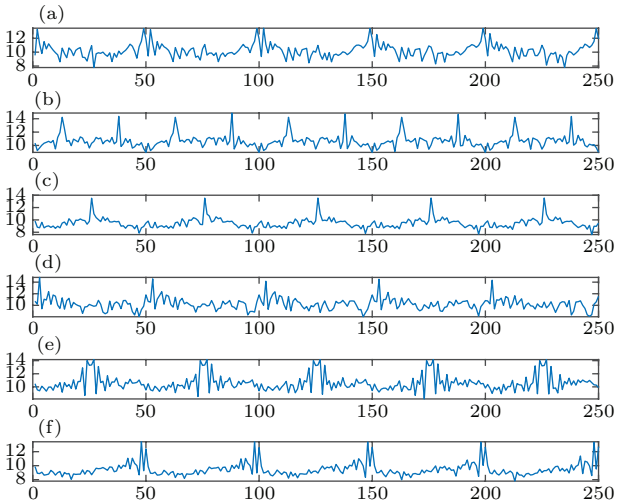


Fig. 5. Maximum values of the power spectral density function of the output signal under different conditions. (a) Triangular wave LFM signal, $\omega = \omega_{\text{start}}$; (b) triangular wave LFM signal, $\omega_{\text{start}} < \omega < \omega_{\text{end}}$; (c) triangular wave LFM signal, $\omega = \omega_{\text{end}}$; (d) sawtooth wave LFM signal, $\omega = \omega_{\text{start}}$; (e) sawtooth wave LFM signal, $\omega_{\text{start}} < \omega < \omega_{\text{end}}$; (f) sawtooth wave LFM signal, $\omega = \omega_{\text{end}}$.

Figure 5 shows the maximum estimation values of the power spectral density function of the Duffing oscillator output signal when the reference frequency is $\omega_{\text{start}} \leq \omega \leq \omega_{\text{end}}$. We set $k = 0.5$, $F = F_{\text{c}} = 0.8259$, $f = 100$ MHz, 125 MHz, 150 MHz, $A = 1$ V, the modulation frequency $f_{\text{M}} = 100$ kHz, $f_{\text{start}} = 100$ MHz, and $f_{\text{end}} = 150$ MHz.

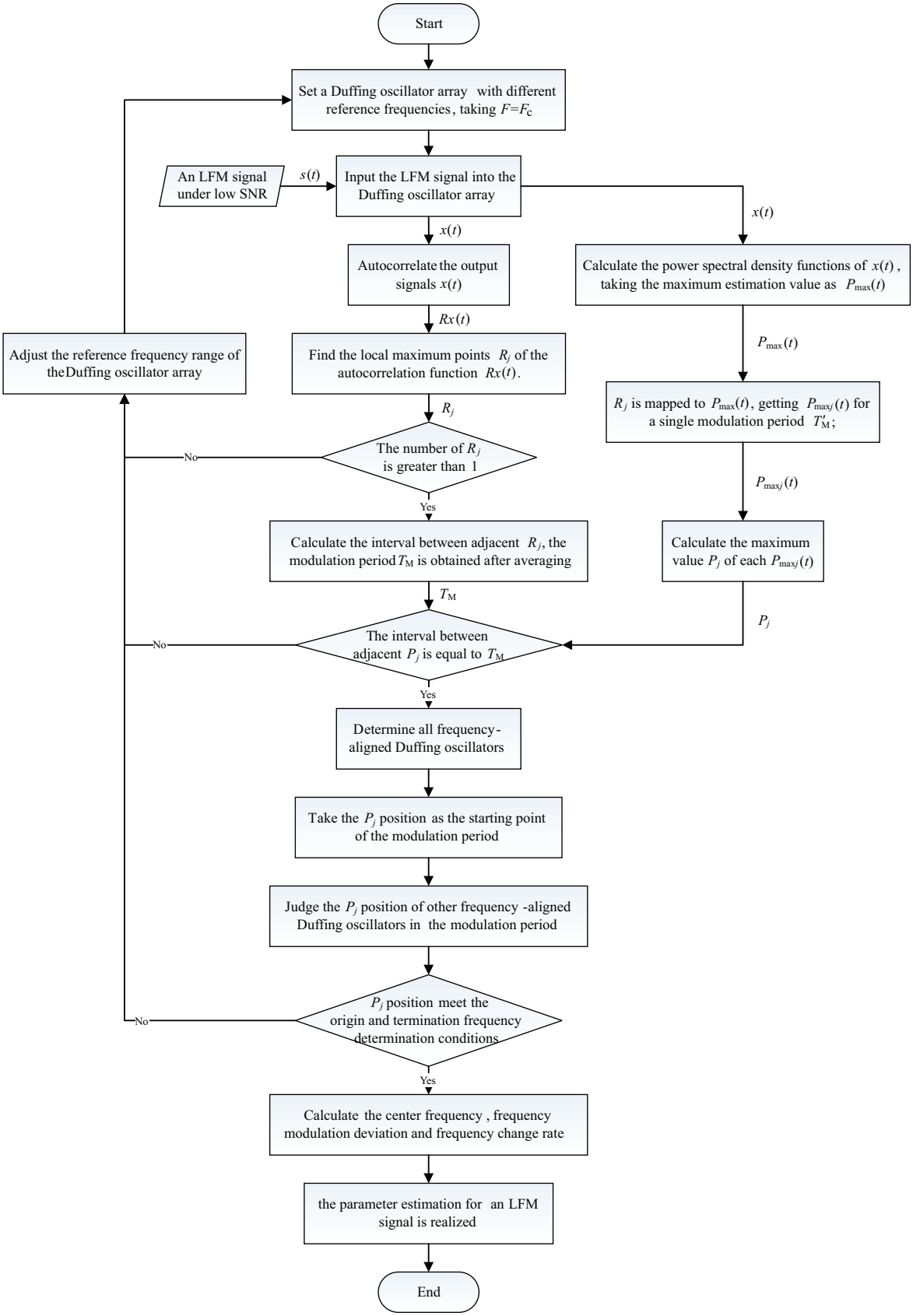


Fig. 6. Flow chart of the parameter estimation method for the LFM signal based on frequency periodicity with low SNR.

According to Figs. 5(a) and 5(d), in a single modulation period, if $\omega = \omega_{\text{start}}$, for the output signal of the Duffing oscillator excited by either the triangular wave or the sawtooth wave LFM signal, its periodic maximum power spectrum estimation value appears at the beginning of each period; if $\omega = \omega_{\text{end}}$, for the output signal of the Duffing oscillator excited by the triangular wave LFM signal, the periodic maximum power spectrum estimation value appears in the middle of each period, while for the output signal of the Duffing oscillator excited by the sawtooth wave LFM signal, the periodic maximum power spectrum estimation value appears at the end of each period. Through the interval and position of the periodic maximum estimation value of the power spectrum, we can find the frequency-aligned Duffing oscillators whose reference frequency is within the frequency range of the LFM signal, and then the origin and termination frequency of the LFM signal can be determined. Finally, the parameter estimation of the LFM signal is completed.

In summary, the process of parameter estimation for the LFM signal based on frequency periodicity under low SNR is as follows:

1) Set a Duffing oscillator array with different reference frequencies, taking $F = F_{\text{c}}$.

2) Input the LFM signal to be measured, and then autocorrelate the output signals $x(t)$ of all Duffing oscillators and obtain $Rx(t)$ after taking the envelope.

3) Find the local maximum points of the autocorrelation function $Rx(t)$. If the number of local maximum points is greater than 1, it can be considered that the reference frequency of the Duffing oscillator meets $\omega_{\text{start}} \leq \omega \leq \omega_{\text{end}}$. The modulation period T_{M} of the LFM signal can be calculated from the interval between adjacent local maximum points.

4) Calculate the power spectral density functions of the output signal $x(t)$ in sections and then take the maximum estimation value as $P_{\text{max}}(t)$.

5) Map the local maximum point of $Rx(t)$ to $P_{\text{max}}(t)$, obtaining the corresponding modulation period T'_{M} and $P_{\text{maxj}}(t)$ for a single modulation period T'_{M}.

6) Calculate the maximum value P_j of each $P_{\text{maxj}}(t)$ and its position in $P_{\text{maxj}}(t)$, respectively. If the interval between adjacent P_j is equal to T'_{M}, the reference frequency of the Duffing oscillator meets $\omega_{\text{start}} \leq \omega \leq \omega_{\text{end}}$.

7) Combined with the results of steps 3) and 6), all frequency aligned Duffing oscillators are determined. Find the one whose reference frequency is the smallest and take the position of P_j as the starting point of the modulation period.

8) We further judge the P_j position of other frequency-aligned Duffing oscillators in the modulation period. If the origin and termination frequency determination conditions of the LFM signal are met, the center frequency, frequency modulation deviation and frequency change rate of the LFM signal can be obtained. In contrast, it is necessary to change the internal reference signal frequency of the Duffing oscillator array and return to step 1) to execute again.

The specific flow chart is shown in Fig. 6.

3.3. Applicability analysis

Combined with the analysis in Subsection 3.1, the parameter estimation method for the LFM signal based on frequency periodicity proposed in Subsection 3.2 estimates the parameters of the LFM signal only related to the strength of the measured signal and SNR. To further analyze the scope of applicability of this method to the spectrum estimation of LFM signals, the frequencies of triangular wave LFM signals are estimated at different frequency change rates, and the results are shown in Table 3. Because this method needs to use the periodic change characteristic of the frequency of the measured LFM signal, the length of the measured signal must be at least equal to double the modulation period. Therefore, the modulation frequency f_{M} and center frequency f_0 are fixed, and only the frequency modulation deviation ΔF_{M} is changed to control the frequency change rate k_{f}. In addition to the parameters listed in Table 3, we set $k = 0.5$, $F = F_{\text{c}} = 0.8259$, and $A = 1$ V.

Table 3. Estimation results of triangular wave LFM signals at different frequency change rates.

f_{M} (kHz)	f_0 (MHz)	Estimation results (MHz)	Frequency modulation deviation $\Delta F_{\text{M}}/f_0$											
			0.02	0.03	0.04	0.05	0.1	1	4	4.1	4.2	4.3	4.4	4.5
0.1	0.1	f_{start}	–[a]	–	–	○[b]	○	○	○	○	○	○	○	–
		f_{end}	–	–	–	○	○	○	○	○	○	○	○	–
1	1	f_{start}	–	–	–	○	○	○	○	○	–	○	–	–
		f_{end}	–	–	–	○	○	○	○	○	–	○	–	–
10	10	f_{start}	–	○	○	○	○	○	○	○	–	○	–	–
		f_{end}	–	○	○	○	○	○	○	○	–	○	–	–
100	100	f_{start}	–	○	○	○	○	○	○	○	○	○	–	–
		f_{end}	–	○	○	○	○	○	○	○	○	○	–	–

[a]The frequency cannot be measured. [b]The frequency can be measured.

The frequency change rate k_{f} is normalized under different modulation frequencies f_{M}. According to the analysis in Table 3, when $0.05 \leq k_{\text{f}} \leq 4.1$, this method can obtain accurate estimation results. When $k_{\text{f}} > 4.1$, due to the rapid change in frequency and the extremely short existence time of the periodic state, it is difficult to meet the duration required for phase

state distinguishment by the power spectrum method, resulting in the failure of frequency identification. When $k_f < 0.05$, because there is a frequency measurement range of $(1 \pm 0.03)\ \omega$ for the traditional Duffing oscillator, i.e., difference frequency $0 < |\Delta\omega| \leq 0.03\omega$, the Duffing oscillator performs intermittent chaotic motion, so all Duffing oscillators within the frequency range of the LFM signal can always perform intermittent chaotic motion. At this time, if the output signal is analyzed by the power spectrum method, there is an uncertain shift in the position of the local maximum point in a single modulation period, which will lead to large errors in the results. This method is also no longer applicable to the measurement of frequency range.

In addition, the frequency of the sinusoidal FM signal also meets the periodic variation characteristic, so the method proposed in this paper is feasible for estimating the modulation period of the sinusoidal FM signal, but its frequency change rate k_f will change with time, and there are extreme cases where $k_f = 0$ and $k_f = \pm\infty$, so it is difficult to use the proposed method to measure the frequency range.

4. Simulation experiment

4.1. Contrastive analysis

Experiment 1 Set $A = 1$ V, $f_M = 0.1$ Hz, $k_f = 1$ Hz/s, $f_0 = 20$ Hz, $f_s = 256$ Hz, $k = 0.5$, $F = F_c = 0.8259$, $f = 5$ Hz, 10 Hz, 15 Hz, 20 Hz, 25 Hz. The parameter estimation results when SNR $= -18 \sim -10$ dB of the Duffing method and the PCFCRD[10] are shown in Fig. 7.

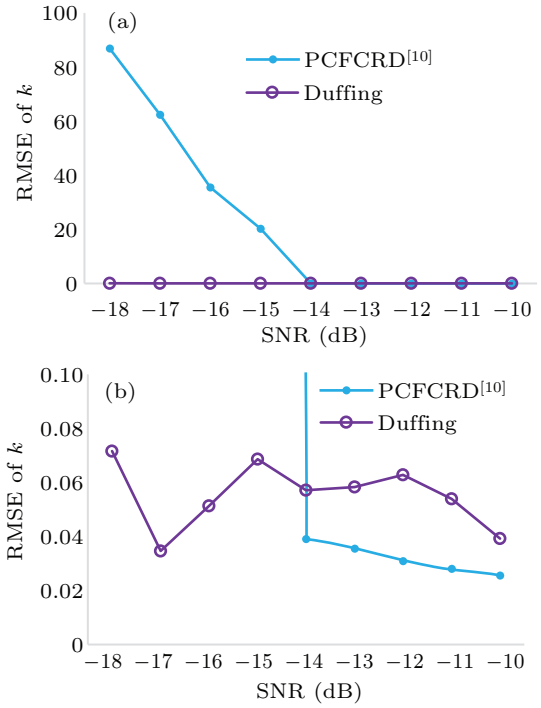


Fig. 7. Root mean square error (RMSE) of the frequency change rate for the LFM signal by two methods with different SNRs: (a) axis range $= 0 \sim 100$; (b) axis range $= 0 \sim 0.1$.

Compared with the PCFCRD, the Duffing method proposed in this paper has better noise immunity and stability for the parameter estimation of LFM signals, so it has great advantages in a low-SNR environment. Although the estimation accuracy under high SNR is not as good as that of PCFCRD, the estimation accuracy at -15 dB is much higher than that of PCFCRD. At the same time, the estimation results are stable with an SNR of $-18 \sim -10$ dB and basically unaffected by noise.

Considering the computational complexity, PCFCRD needs to search the peak value of the signal energy in the centroid frequency–chip rate (CFCR) domain, which is blind and requires a large amount of computation. In contrast, the Duffing method proposed in this paper avoids a one-dimensional search process, thereby saving computational effort.

Experiment 2 Comparing the parameter estimation results of the proposed method with the ℓ^p-norm method,[16] the root mean square error (RMSE) of the parameter estimation results, including the frequency change rate and center frequency, by the two methods under different SNRs are shown in Fig. 8. The signal parameters are $A = 1$ V, $f_M = 1$ Hz, $k_f = 100$ Hz/s, $f_0 = 200$ Hz, and sample frequency $f_s = 8000$ Hz. The Duffing oscillator relevant parameters are $k = 0.5$, $F = F_c = 0.8259$, $f = 100$ Hz, 150 Hz, 200 Hz, 250 Hz, and 300 Hz. Because the ℓ^p-norm method has good noise robustness only when the SNR ≥ -5 dB and its detection accuracy decreases significantly when the SNR falls below -5 dB, only the estimation results when the SNR ≥ -5 dB are compared.

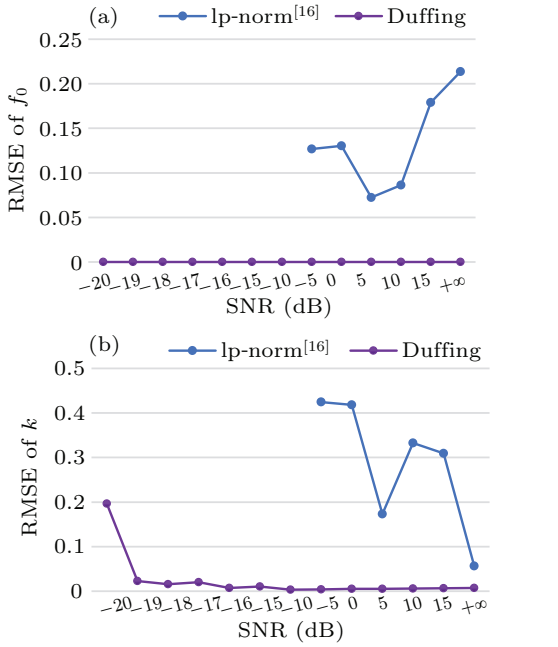


Fig. 8. RMSE of parameter estimation for the LFM signal by two methods with different SNRs: (a) RMSE of the center frequency; (b) RMSE of the frequency change rate.

The parameter estimation results of the proposed method with the Duffing oscillator based on frequency periodicity in this paper are obviously better than those of the ℓ^p-norm method, regardless of the estimation accuracy or stability. The estimation accuracy differences at -19 dB and 15 dB are small.

In order to verify the computational complexity of this method, the computing times for the Duffing method and ℓ^p-norm method are shown in Table 4. The simulation results show that the calculation time of the Duffing method is not much different from that of the ℓ^p-norm method, and even slightly less.

Table 4. Computing time of two methods.

Method	Computing time (s)
ℓ^p-norm	2.192
Duffing	1.628

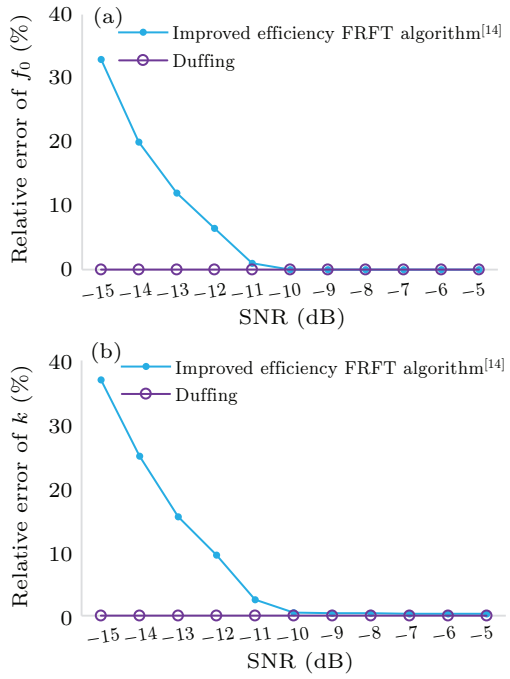


Fig. 9. RE of parameter estimation for the LFM signal by two methods with different SNRs: (a) RE of the center frequency; (b) RE of the frequency change rate.

Experiment 3 Set the signal parameters $A = 1$ V, $f_M = 1$ Hz, $k_f = 1000$ Hz/s, $f_0 = 1500$ Hz, and $f_s = 5000$ Hz and the Duffing oscillator parameters $k = 0.5$, $F = F_c = 0.8259$, and $f = 1000$ Hz, 1500 Hz, 2000 Hz, 2500 Hz, and 3000 Hz. Comparing the parameter estimation results of the Duffing method with the efficient FRFT improved search algorithm,[14] the relative error (RE) of the center frequency and frequency change rate by the two methods with different SNRs are shown in Fig. 9. Because the FRFT algorithm is no longer applicable when SNR $= -15$ dB, we only compare the estimation results with SNRs of $-15 \sim 5$ dB.

There is little difference in parameter estimation accuracy between the improved efficiency FRFT algorithm and the proposed method in this paper at high SNRs, but the proposed method has obvious advantages at low SNRs. In addition, its estimation of f_0 and k_f is relatively stable, while the estimation accuracy of the FRFT algorithm decreases significantly under -11 dB.

The computing time for the Duffing method and efficient FRFT improved search algorithm is shown in Table 5. Although the calculation time of the Duffing method is more than that of the efficient FRFT improved search algorithm, it is still a simple and efficient method with lower computational cost.

Table 5. Computing time of two methods.

Method	Order error	Computing time (s)
FRFT	0.01	0.101
	0.01	0.138
	0.001	0.192
Duffing	–	1.526

4.2. Weak LFM signal detection with low SNR

To further verify the effect of the method proposed in Section 3 on the parameter estimation of weak LFM signals with low SNR, simulation experiments are carried out. The parameters to be measured mainly include the modulation frequency, center frequency and frequency change rate of triangular wave and sawtooth wave LFM signals.

Table 6. Parameter estimation results of the LFM signal with different SNRs.

SNR (dB)	Triangular wave					Sawtooth wave				
	T_M (μs)	f_M (kHz)	f_0 (MHz)	k_f		T_M (μs)	f_M (kHz)	f_0 (MHz)	k_f	
				Value (GHz·s^{-1})	Error (%)				Value (GHz·s^{-1})	Error (%)
$+\infty$	9.9999	100.00	125	10000	0	9.9999	100.00	125	5000.0	0
0	9.9999	100.00	125	10000	0	9.9999	100.00	125	5000.0	0
−10	9.9999	100.00	125	10000	0	10.001	99.991	125	4999.6	0.008
−20	9.9999	100.00	125	10000	0	9.9999	100.00	125	5000.1	0.002
−25	9.9980	100.02	125	10002	0.02	9.9999	100.00	125	5000.1	0.002
−26	10.017	99.832	125	9983.2	0.168	9.9999	100.00	–	–	–
−27	9.6900	103.20	–	–	–	9.6466	103.66	–	–	–

An array composed of five Duffing oscillators with different frequencies of the internal reference signal is constructed, setting $k = 0.5$ and $F = F_c = 0.8259$, and the initial reference frequencies f are set to 75 MHz, 100 MHz, 125 MHz, 150 MHz and 175 MHz. The parameters of the input signal to be measured are set as follows: $A = 0.05$ V, $f_M = 100$ kHz, $f_0 = 125$ MHz, $f_s = 10$ GHz, triangular wave $k_f = 10^4$ GHz·s^{-1}, and sawtooth wave $k_f = 5000$ GHz· s^{-1}.

In this paper, the SNR detection threshold is obtained by adjusting the noise strength. When the signal amplitude $A = 0.05$ V, the noise strength is taken as $\sigma^2 = 0.00125$, 0.0125, 0.125, 0.395, 0.5, and 0.6265, and corresponding SNRs of 0 dB, −10 dB, −20 dB, −25 dB, −26 dB, and −27 dB are obtained. According to the steps in Subsection 3.2, the simulation is carried out with different SNRs, and the parameter estimation results of the LFM signal are shown in Table 6.

Experiments show that the proposed method in this paper can effectively estimate the modulation frequency, center frequency and frequency change rate of LFM signals with different SNRs, and the SNR detection threshold can reach −25 dB. Compared with the triangular wave LFM signals, the sawtooth wave LFM signals have a sudden change in frequency from the termination frequency to the origin frequency between every two modulation cycles, which will result in a sudden change in the motion state of the Duffing oscillator. At this time, if the power spectrum method is used to distinguish the motion state of the Duffing oscillator, there may be an error in the frequency estimation of the LFM signal because this method uses the average power spectrum estimation value in a period of time as the judgment basis. Therefore, the parameter estimation of the triangular wave LFM signal is better than that of the sawtooth wave LFM signal. Although the detection accuracy decreases at −26 dB, the relative error of the frequency change rate is only 0.168%, and higher-accuracy parameter estimation results can still be obtained.

5. Conclusion

In this paper, we have analyzed the relationship between the output signals of the Duffing oscillator and the input periodic signals with different frequencies. Then, based on the periodic variation characteristics of the output signal of the Duffing oscillator excited by the LFM signal, this paper proposes a parameter estimation method for the LFM signal with a Duffing oscillator based on frequency periodicity. This method utilizes the periodic change in the Duffing oscillator output signal with the frequency change in the LFM signal to estimate the modulation period first, and then the periodic power spectrum method is used to distinguish the motion state of the Duffing oscillator. The relationship between the reference frequencies of frequency-aligned Duffing oscillators and the frequency range of the LFM signal is determined. Furthermore, the estimated values of the central frequency, frequency deviation and frequency change rate of the LFM signal are also obtained. Therefore, high-accuracy parameter estimation for the LFM signal at −25 dB SNR is realized.

Acknowledgement

Project supported by the National Natural Science Foundation of China (Grant No. 61973037).

References

[1] Wang C H, Shao W J and Ju Y 2020 *Shipboard Electron. Count.* **43** 76
[2] Boashash B and Ouelha S 2018 *Digit. Signal Prog.* **77** 120
[3] Diao M, Zhu Y F, Ning X Y and Wang Z D 2022 *J. Harbin Insti. Technol.* **54** 88
[4] Jing F L, Zhang C J, Si W J, Wang Y and Jiao S H 2019 *J. Xidian Uni.* **46** 102
[5] O'Shea P 2002 *IEEE Signal Process. Lett.* **9** 251
[6] O'Shea P 2004 *IEEE Signal Process. Lett.* **52** 385
[7] Wang P and Yang J Y 2006 *Digit. Signal Prog.* **16** 654
[8] Wang P, Li H B, Djurović I and Himed B 2010 *IEEE Trans. Aerospace Electron. Syst.* **46** 963
[9] Li D, Zhan M Y, Su J, Liu H Q, Zhang X P and Liao G S 2017 *IEEE Trans. Geos. Remote Sens.* **55** 6402
[10] Zheng J B, Liu H W and Liu Q H 2017 *IEEE Trans. Signal Process.* **65** 6435
[11] Almeida L B 1994 *IEEE Trans. Signal Process.* **42** 3084
[12] Qi L, Tao R, Zhou S Y and Wang Y 2003 *Sci. Chin. Ser. E* **33** 749
[13] Huang X, Tang S Y, Zhang L R and Gu Y B 2017 *J. Electron. Inf. Technol.* **39** 2905
[14] Liu L M, LI H X, LI Q, Han Z Z and Gao Z B 2021 *J. Electron. Inf. Technol.* **43** 2798
[15] Liu X L, Han J, Wang C Y and Xiao B 2019 *Optik* **182** 529
[16] Guo Y, Zhang X W and Yang L D 2021 *Optik* **239** 166681
[17] Wang K, Yan X P, Zhu Z Q, Hao X H, Li P and Yang Y 2020 *Sensors* **20** 6412
[18] Wang G Y, Chen D J, Lin J Y and Chen X 1999 *IEEE Trans. Ind. Electron.* **46** 440
[19] Aledealat K, Khasawinah K, Obeidat A, Gharaibeh M, Jaradat A, Hasan M K Qaseer and Rousan A A 2018 *AIP Adv.* **8** 095102
[20] Zhu Z Q, Hou J, Yan X P, Li P and Hao X H 2019 *J. Beijing Uni. Aero. Astro.* **45** 2069
[21] Liu B and Liu J M 2001 *J. Electron. Meas. Instrum.* **15** 41
[22] Zhang Q J, Han X L and Liu J 2017 *Spacecraft Eng.* **26** 1
[23] Springer A, Pohl A, Gugler W, Huemer M, Reindl L, Ruppel C C W, Seifert F and Weigel R 1998 *IEEE MTT-S International Microwave Symposium Digest*, June 07–12, 1998, Baltimore, MD, USA
[24] Gao F, Yin H S and Zhang C X 2011 *Appl. Electron. Tech.* **37** 95